Pulsed photoacoustic Doppler flowmetry using a cross-correlation method

J. Brunker and P. Beard
Department of Medical Physics and Bioengineering, University College London, Gower Street, London, WC1E 6BT, United Kingdom
http://www.medphys.ucl.ac.uk/research/mle/index.htm

ABSTRACT

The feasibility of making spatially resolved measurements of blood flow using pulsed photoacoustic Doppler techniques has been explored. Doppler time shifts were quantified via cross-correlation of pairs of photoacoustic waveforms generated within a blood-simulating phantom using pairs of laser light pulses. The photoacoustic waves were detected using a focussed or planar PZT ultrasound transducer. This approach was found to be effective for quantifying the linear motion of micron-scale absorbers imprinted on an acetate sheet moving with velocities in the range 0.15 to 1.50 ms^{-1}. The effect of the acoustic spot diameter and the time separation between the laser pulses on measurement resolution and the maximum measurable velocity is discussed. The distinguishing advantage of pulsed rather than continuous-wave excitation is that spatially resolved velocity measurements can be made. This offers the prospect of mapping flow within the microcirculation and thus providing insights into the perfusion of tumours and other pathologies characterised by abnormalities in flow status.

Keywords: photoacoustic imaging, pulsed, Doppler, flow, cross-correlation

1. INTRODUCTION

Photoacoustic imaging relies upon the use of laser generated ultrasound to produce optical absorption based images of soft tissues [1]. Endogenous image contrast is dominated by haemoglobin on account of its strong optical absorption at visible and near infrared wavelengths. As a consequence, photoacoustic imaging is well suited to providing images of vascular anatomy [2, 3]. In addition, by varying the excitation laser wavelength and exploiting the known spectral differences between oxy and deoxy-hemoglobin, measurements of absolute blood oxygen saturation can be made [4]. This ability to characterise the structure and oxygenation status of the vasculature makes the technique well suited to the study of tumours and other pathologies characterised by abnormalities in perfusion and oxygen supply. A further potential functional capability is the measurement of blood velocity using Doppler flowmetry techniques. This would be useful in its own right, for example to study flow in tumour vessels where the tortuous nature of the microvasculature can lead to chaotic and variable blood flow which can inhibit therapeutic response. However, if both blood flow and oxygen saturation can be measured simulataneously there is also the enticing prospect of being able estimate oxygen delivery and thus provide a measure of oxygen consumption – an important physiological parameter that is almost impossible to measure non-invasively using other methods without employing contrast agents.

Photoacoustic flow measurements can be made in a manner analogous to conventional pulse echo Doppler ultrasound – that is to say by recovering the Doppler frequency, phase or time shift encoded on to photoacoustic waves emitted by moving red blood cells. Unlike Doppler ultrasound however, the detected acoustic signal is emitted by the blood cells as opposed to being weakly reflected from them. This offers significant SNR advantages especially when measuring flow in microvessels as these exhibit low echogenicity. Furthermore, Doppler ultrasound measurements of the relatively low flow velocity (<50mm/s) in microvessels can be corrupted by the much larger backscattered signal from the surrounding tissue which can move at comparable speeds due to respiratory or cardiac motion. In photoacoustic Doppler flowmetry this is expected to be less problematic due to the strong optical absorption of blood compared to the constituents of the vessel wall and surrounding tissue.

The basic principles of photoacoustic Doppler flowmetry were first outlined in reference [5]. Subsequently, photoacoustic measurements of flow in a tissue mimicking phantom were obtained by recovering Doppler frequency shifts using CW excitation [6, 7]. However, in common with CW Doppler ultrasound, this approach can not readily provide depth resolved measurements. In this paper we describe a method based upon pulsed excitation that overcomes

Photons Plus Ultrasound: Imaging and Sensing 2010, edited by Alexander A. Oraevsky, Lihong V. Wang,
Proc. of SPIE Vol. 7564, 756426 · © 2010 SPIE · CCC code: 1605-7422/10/$18 · doi: 10.1117/12.841760

this limitation. In this approach photoacoustic waves are generated in moving blood using a series of laser pulses. The flow velocity is then determined by measuring the progressive time shift of the detected photoacoustic signals due to the motion of red blood cells using time-correlation methods. Since the correlation processing can be performed on a segment of the detected time resolved signal corresponding to a specific depth, spatially resolved measurements can be made. Section 2 describes the underlying principles of the technique and section 3 the experimental methods used to evaluate it using a blood tissue phantom. Section 4 discusses the signal processing and statistical methods for estimating the velocity. The experimentally determined velocity measurements, resolution and dynamic range are presented and discussed in section 6.

2. PRINCIPLES OF PULSED PHOTOACOUSTIC DOPPLER FLOWMETRY

The photoacoustic (PA) effect can be exploited to make Doppler flow measurements [1]. Consider a cluster of particles, such as red blood cells, within a vessel as shown in Fig. 1. Following pulsed wide-field optical illumination, photoacoustic waves are generated and subsequently detected using a directional ultrasound receiver acoustically coupled to the tissue surface. Since an extended region of the tissue is illuminated due to the diffuse nature of light transport in tissue, the beam width of the receiver, rather than the illuminated volume, defines the region over which the signals are collected. The excitation laser is operated in pulsed mode; between pulses, the motion of particles within the transducer focal region will produce a change d in the distance travelled by the signals to the detector, and this produces a difference t_s in the signal arrival times. This measured time shift is related to the speed of sound c in the medium and the angle θ between the direction of particle motion and the axis of the transducer receive beam:

$$t_s = \frac{d}{c} = \frac{l\cos\theta}{c} \tag{1}$$

l is the distance travelled by the particles between successive laser pulses, which are separated by a time T. The velocity of particles V is then given by

$$V = \frac{l}{T} \tag{2}$$

which, using Eq. (1), can then be written

$$V = \frac{ct_s}{T\cos\theta} \tag{3}$$

This is analogous to the Doppler equation derived for pulse-echo ultrasound [8].

The cross-correlation function can be used to determine the time shift t_s between two ultrasound waveforms. For continuous functions, f and g, the cross-correlation is defined as:

$$(f \star g)(t) = \int_{-\infty}^{\infty} f^*(\tau)\, g(t+\tau) d\tau \tag{4}$$

where f^* is the complex conjugate of f.

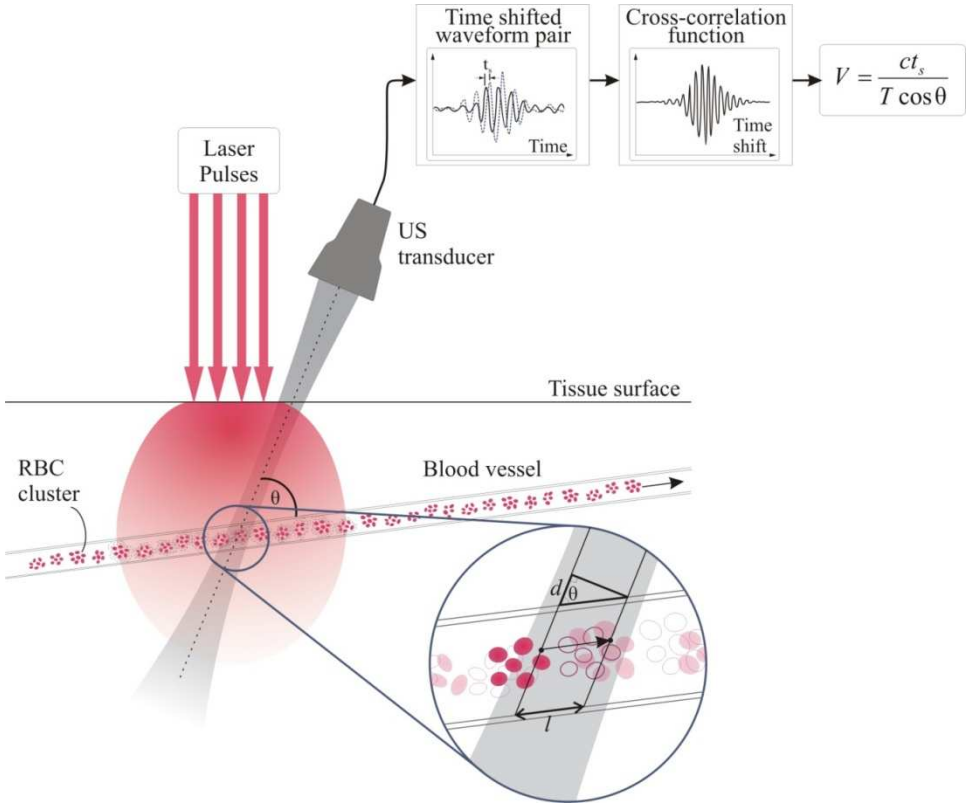

Fig. 1. Schematic showing the detection of time-shifted photoacoustic signals. The signals are generated from clusters of moving red blood cells (RBCs) illuminated with an excitation laser pulsing at a frequency 1/*T*. The insert shows the distribution of RBCs (represented by solid ellipses) when a particular laser pulse is fired, and the new positions (unfilled ellipses) coincident with the firing of the second pulse a time *T* later. Between the pulses the cells have moved a distance *l* along the blood vessel.

3. EXPERIMENTAL METHOD

Fig. 2 shows the experimental setup used to demonstrate the technique. A rotating phantom was used to simulate the motion of red blood cells. This comprised a wheel mounted on the axle of a DC electric motor. The wheel consists of a Perspex disc overlaid with a sheet of acetate imprinted around the rim with a non-uniform, random pattern of light-absorbing micron-scale dots. Two laser beams were aligned in a tank of water so that both illuminated the same region (about 2 cm in diameter) near the edge of the wheel, allowing the rotary motion of the dots ("particles") to be approximated to the linear flow of red blood cell clusters. The distribution of the absorbing dots is shown in Fig. 3. The dimensions of the dots are on the order of 10 μm and they cover approximately 90% of the total imprinted area. This is comparable to the diameter and volume fraction of red blood cells which are on average 7.5 μm [9] and about 50% respectively.

Photoacoustic waveform pairs were generated using pairs of laser pulses with pulse separations *T* in the range 0.1 ms to 50 ms. Since most Q-switched lasers only produce sufficient pulse energies (several mJ) at low, fixed pulse repetition frequencies of a few tens of Hz, two Q-switched Nd:YAG lasers emitting at 1064nm were used to produce the pulse pairs. One laser was operated at 20 Hz, and the second laser was triggered off the first after a pre-selected time delay *T*. Both lasers were carefully aligned so that they illuminated the same region of the phantom. Light absorbing particles within the target area emitted a photoacoustic wave each time they were illuminated and these waves were detected using an ultrasound transducer also immersed in the water. The transducer was positioned so that the distance from the illuminated region of the wheel was approximately equal to the transducer focal length; the transducer *x*-, *y*- and *z*-coordinates and angle θ were then adjusted to give the maximum photoacoustic signal. If the position of the particles had

shifted between the two laser pulses then a time shift was observed between the two corresponding photoacoustic waveforms. Signals were acquired using an oscilloscope (DSO-Tektronix TDS784D).

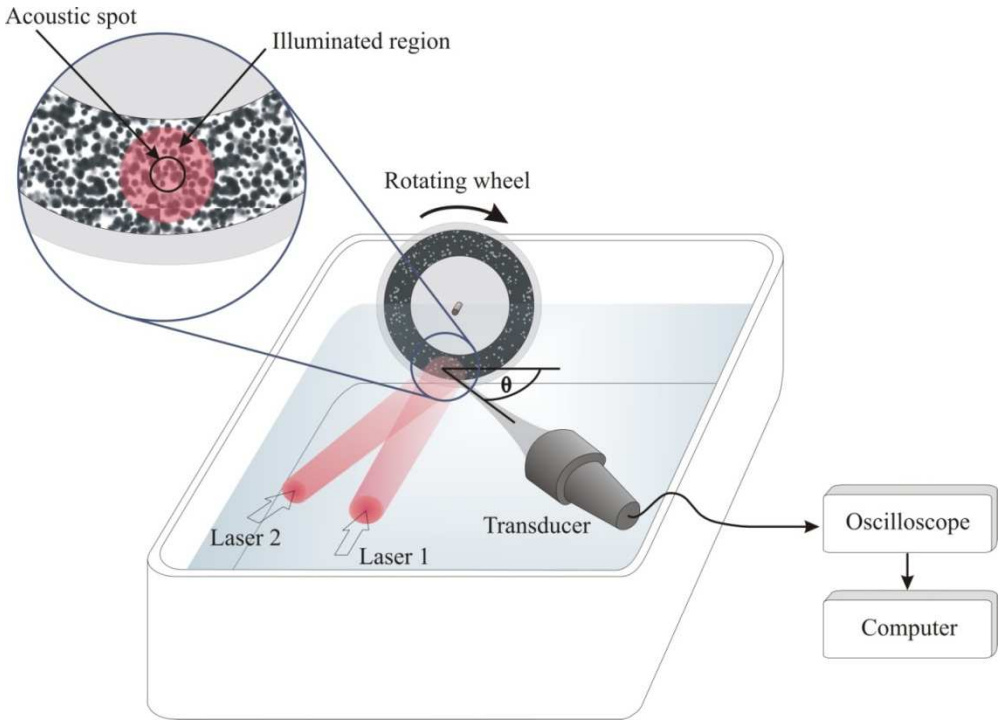

Fig. 2. Experimental setup for pulsed photoacoustic Doppler flow measurement where the motion of micron-scale absorbers imprinted on to the rim of a rotating wheel is used to represent blood flow. Two laser pulses (one emitted by laser 1 and the other by laser 2) separated by a time *T* are used to generate a pair of acoustic waveforms. Each laser pulse triggers the oscilloscope via a photodiode; the photoacoustic signal received by the ultrasound (US) transducer is acquired on a separate channel, and then downloaded to the computer for processing. The insert shows a typical distribution of the micron-scale dots printed onto the wheel phantom. A large area (at least 2 cm) of the absorbers is illuminated, but photoacoustic signals are only collected from the smaller region (about 1 mm) defined by the transducer focal spot.

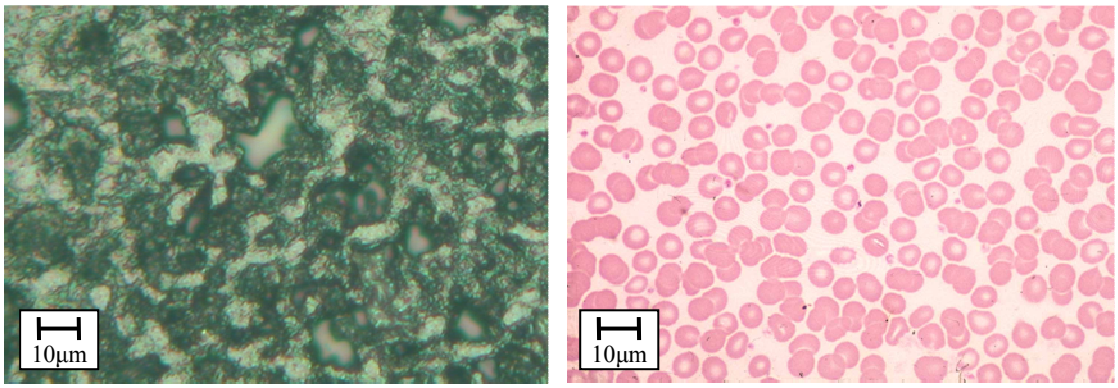

Fig. 3. Comparison of optical microscopy images showing the distribution of absorbers in the phantom (left) and a histological section [10] containing red blood cells (right). The scale bars are only approximate, but it is clear that the "particle" dimensions and densities in both images are comparable. In the phantom the "particles" comprise micron-scale dots printed onto an acetate sheet.

4. SIGNAL ACQUISITION AND PROCESSING

Series of 25 successive waveform pairs (50 frames of 1000 points in length) were captured in real time using the FastFrame™ Segmented Memory feature of the oscilloscope. This enabled the waveforms to be concatenated in a single record and downloaded to a PC where cross-correlation (Eq. (4)) of each pair of photoacoustic waveforms allowed measurement of the time shift between them and hence calculation of the velocity (Eq. (3)) of the particles. Calculations for all 25 pairs resulted in a distribution of velocities from which the mode was extracted. The perfect histogram of velocity measurements would consist only of data points clustered around the modal value. However, every data set contained some waveform pairs that were poorly correlated resulting in velocity estimates that differed considerably from the mode. These outlying values were rejected and the standard deviation of the reduced data set was used as the measurement uncertainty.

This procedure was repeated for different speeds in order to determine the capability of the technique for estimating velocities within the range 0.15 ms^{-1} to 2.00 ms^{-1}. Below 0.15 ms^{-1} the speed of the motor was non-uniform, and above 2 ms^{-1} turbulence in the water bath distorted the measured signal. The angular velocity of the wheel phantom was obtained using the spokes of a wheel mounted behind the Perspex disc: the spokes periodically intercepted the light emitted by an LED that was incident on a photodiode resulting in a square waveform signal with a period measured on a second oscilloscope. Calculation of the linear velocity from the angular velocity required measurement of the radial distance R from the wheel centre to the centre of the focal region of the transducer. Errors in the linear velocity were estimated from the variation in the square waveform on the second oscilloscope and the estimated radial distance R of 37 ± 1 mm. The velocity values obtained using this method were regarded as the "known" values and compared with those acquired via cross-correlation of the PA waveform pairs.

5. RESULTS AND DISCUSSION

Results acquired for velocities between 0.20 ms^{-1} and 1.35 ms^{-1} using a 20 MHz planar transducer (Fig. 4) show close agreement with the known values until velocities of about 1.0 ms^{-1} are exceeded. In general, with increasing velocity there is an increase in the y error bars due to increasing lack of correlation. The following sub-sections discuss the influence of the time separation T between the laser pulses and the acoustic spot size of the transducer on a) the maximum measured velocity and b) the resolution of the measurements (indicated by the size of the error bars).

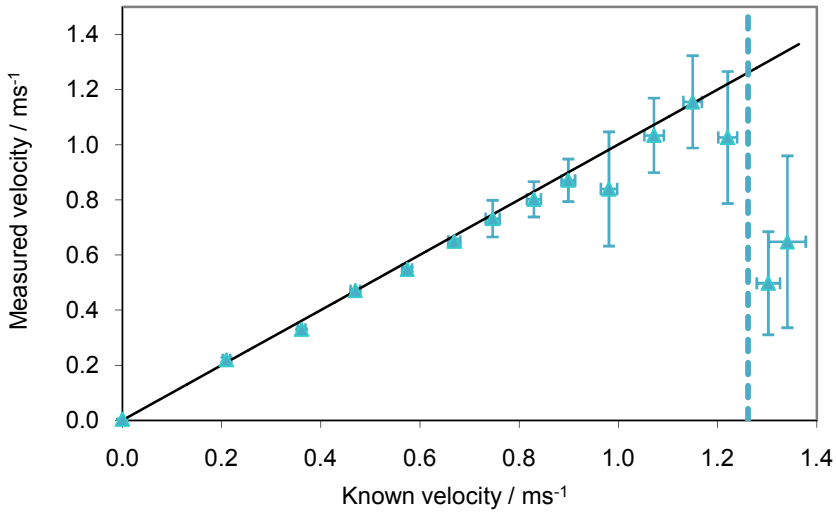

Fig. 4. Comparison of velocity values calculated from the time-shifted photoacousic waveform pairs with the known velocity of the absorbers. This data was acquired using a 20 MHz planar transducer and the time separation between the laser pulses was 1.0 ms. Correlation is lost for velocities beyond that marked by the dashed line. Each data point is the mean of at least two modal values of data sets containing 25 waveform pairs. Measurements more than 1 standard deviation from the modal value were excluded, and errors in the measured velocities were estimated using the standard deviation of this "mode-trimmed" data set.

5.1 Upper velocity limits

Reductions in both accuracy and precision can be attributed to loss of correlation due to the movement of a particular region entirely out of the focal spot by the time the second laser pulse is emitted. The limiting speed $|V_{\max}|$ (metres per second) beyond which this occurs can be calculated from the acoustic spot diameter (w in millimetres) and the pulse separation (T in milliseconds):

$$|V_{max}| = \frac{w_p}{T} = \frac{w}{T \sin\theta} \tag{5}$$

The geometrical relationship between w and w_p is illustrated in Fig. 5.

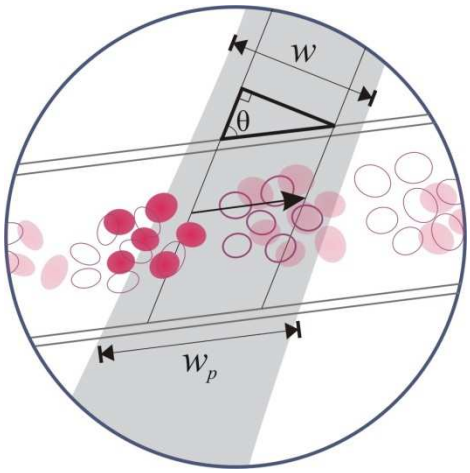

Fig. 5. Alignment of the transducer axis at an angle θ relative to the flow direction. The acoustic spot diameter w results in acquisition of signals from a length w_p of the vessel.

The dashed line in Fig. 4 indicates the maximum accurately measured velocity, which was estimated by taking the mean of the two measured velocities on either side of this observed "cut-off". Fig. 6 shows that the measured cut-off values for three different values of T agree well with calculations of $|V_{\max}|$ using Eq. (5).

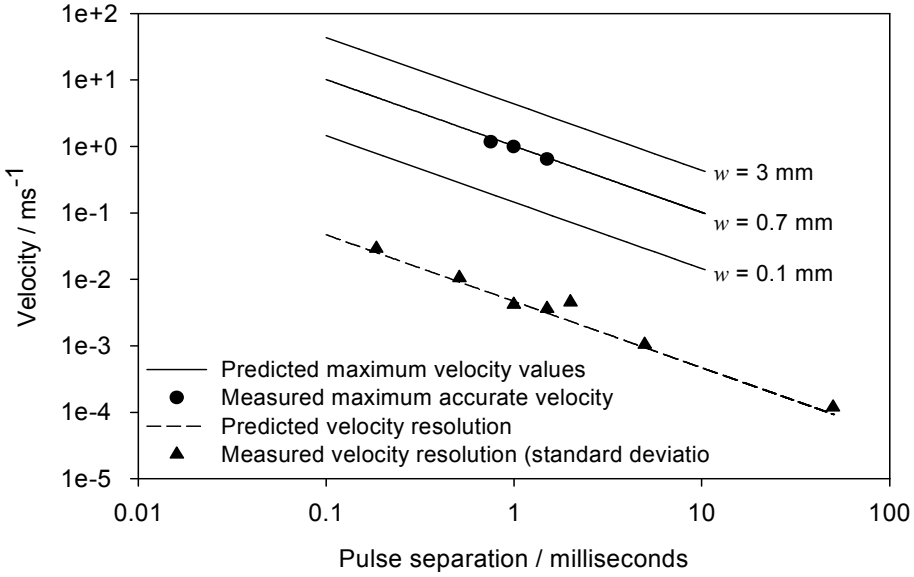

Fig. 6. Scalability of maximum measurable velocity ($|V_{max}|$) and velocity resolution ($\pm\delta V/2$) with pulse separation. $|V_{max}|$ is also dependent on the acoustic spot size (w) and calculations for w = 0.1 mm, 0.7 mm and 3 mm are displayed using solid lines. The circular data points correspond to the maximum accurately measured velocities beyond which data points were observed to drop off significantly from the expected trend line. These pulsed photoacoustic Doppler flow measurements were made using a 5 MHz focussed transducer with an acoustic spot diameter w of 0.7 mm, positioned at an angle θ of about 47° relative to the rotation of a medium density wheel phantom (dots covering about 70% of the total imprinted area); three data sets were acquired with pulse separations of 0.75 ms, 1.0 ms and 1.5 ms. The triangular data points show the standard deviations of velocity distributions obtained using seven different laser pulse separations. A 20 MHz ultrasound transducer was used to detect the photoacoustic signals generated from the high density wheel phantom. The dashed line shows the resolution values predicted using Eq.(8).

5.2 Resolution limits

The smallest detectable time shift δt_s is ultimately limited by the temporal sampling interval of the oscilloscope. If both c and θ are fixed then, from Eq. (3), it is clear that the smallest detectable velocity δV and the time separation T between the laser pulses are inversely proportional:

$$\delta V \times T = \frac{c\delta t_s}{\cos\theta} = \text{constant} \tag{6}$$

Taking c =1500 ms^{-1} and θ = 50°, then, for δt_s = 4 ns,

$$\delta V \times T = \frac{1500\,\text{ms}^{-1}\times 4\times 10^{-9}}{\cos(50°)} \approx 9.33\times 10^{-6}\text{m} \tag{7}$$

This means that for a particular pulse separation T there is a fundamental resolution limit of $\pm\,\delta V/2$:

$$\frac{\delta V}{2} \approx \frac{4.67\times 10^{-6}\text{m}}{T} \tag{8}$$

A series of measurements were made using seven different pulse separations, and the resolution $\pm\delta V/2$ calculated from Eq. (8) was compared with the standard deviation of each distribution of measured velocities. To obtain the measured data, the phantom was held stationary in order to avoid the influence of variations in the speed of the dc motor. As shown in Fig. 6, the predicted and measured resolution estimates are well-matched, indicating that it is the sampling interval of oscilloscope rather than timing jitter in the synchronisation of the two lasers that dominates the measurement resolution.

6. CONCLUSION

It has been shown that a photoacoustic time shift due to moving particles can be measured via cross-correlation of pairs of photoacoustic waveforms generated using pulsed lasers and detected using an ultrasound transducer. This pulsed photoacoustic Doppler technique has proved effective for making velocity measurements over a range of approximately 0.15 to 1.50 ms^{-1} using phantoms in which the particle dimensions and densities were comparable to those of red blood cells. This is a critical requirement for the in vivo implementation of the technique: if the density of absorbers is sufficiently high to approximate to a continuum, the two constituent waveforms within a pair will appear identical and no time shift will be observed. Whether this will be the case with blood as a target remains to be seen but these results and the successful demonstration of cross correlation pulse-echo ultrasound measurements of blood flow [11] suggest a degree of optimism is warranted. The accuracy and resolution of the velocity measurements are scalable with the time separation between the laser pulses and the acoustic spot size of the transducer: a pulse separation of 5 ms and acoustic spot size of 0.7 mm would allow velocities up to a maximum of about 180 mm/s to be measured with a resolution of about ±1 mm/s; increasing the pulse separation to 50 ms would limit the range to velocities below 18 mm/s but give a resolution of ±0.1 mm/s. Therefore, appropriate choice of these parameters would allow precise, spatially resolved quantification of low flow speeds such as that of blood in the microcirculation.

REFERENCES

[1] Xu M., Wang, L.V., "Photoacoustic imaging in biomedicine", Review of Scientific Instrument 77(4), 041101 (2006)

[2] Zhang, E. Z., Laufer, J. G., Pedley, R. B., and Beard, P. C., "In vivo high-resolution 3D photoacoustic imaging of superficial vascular anatomy," Physics in Medicine and Biology 54(4), 1035-1046 (2009).

[3] Zhang, H. F., Maslov, K., Stoica, G. and Wang, L., H., V., "Functional photoacoustic microscopy for high-resolution and noninvasive in vivo imaging" Nature Biotechnology 24(7), 848-51(2006).

[4] Laufer, J. G., Delpy, D., Elwell, C., and Beard, P. C., "Quantitative spatially resolved measurement of tissue chromophore concentrations using photoacoustic spectroscopy: application to the measurement of blood oxygenation and haemoglobin concentration," Physics in Medicine and Biology 52(1), 141-168 (2007).

[5] Beard, P. C., "Flow velocity measurements," UK Patent Application WO 03/039364 (2001).

[6] Fang, H., Maslov, K. and Wang, L.V., "Photoacoustic Doppler flow measurement in optically scattering media," Applied Physics Letters 91(26), 264103 (2007).

[7] Fang, H., Maslov, K. and Wang, L.V., "Photoacoustic doppler effect from flowing small light-absorbing particles," Physical Review Letters 99(18), 184501 (2007).

[8] Foster, S. G., Embree, P. M. and Obrien, W. D., "Flow velocity profile via time-domain correlation error analysis and computer-simulation," IEEE Transactions on Ultrasonics Ferroelectrics and Frequency Control 37(3), 164-17 (1990).

[9] Bain, B., [Morphology of Blood Cells in Blood Cells: A Practical Guide], Wiley-Blackwell, 52-154 (2002).

[10] University of Cambridge, Department of Pathology http://www.path.cam.ac.uk/partIB_pract/NHP1/. (cited 08 February 2010).

[11] Embree, P.M. and Obrien, W. D., "Volumetric blood-flow via time-domain correlation - experimental-verification," IEEE Transactions on Ultrasonics Ferroelectrics and Frequency Control 37(3), 176-189 (1990).